

# APPROXIMATE ANALYSIS OF POST-LIMIT RESPONSE OF FRAMES

By K. D. Hjelmstad,<sup>1</sup> Associate Member, ASCE, and S. Pezeshk,<sup>2</sup> Associate Member, ASCE

**ABSTRACT:** An approach to estimating the limit and post-limit behavior of a framed structure from its geometrically linear response is presented. The method follows from a particular restatement of the weak form of the nonlinear differential equations governing the response of the structure, and is based upon the observation that geometric effects are insensitive to redistribution of the moment field in planar framed structures. The formulation gives insight into the relationship between important observed phenomena and the complex nonlinear governing equations. A novel derivation of Horne's method for estimating the nonlinear response of frames is presented and extended to the important case of nonproportional loads. The role of the linearized geometric stiffness matrix, and the buckling eigenvalues is clearly demonstrated. Several examples are given to evaluate the validity of the inherent assumptions and to demonstrate the effectiveness of the approach.

## INTRODUCTION

Elastoplastic structures subjected to gravity loads generally exhibit a limit point with degrading post-limit behavior when subjected to overloads. Thus geometric effects play a fundamental role in determining the maximum capacity of a structure and its rate of failure. Recent advances in computational mechanics have made it possible to carry out fully nonlinear analyses of elastoplastic structures, and effective algorithms exist for tracing limit points and post-limit behavior. However, these methods give little qualitative insight into the behavior of complex structures.

The purpose of the present paper is to describe a method for accounting for the geometric effects in an elastoplastic analysis through a simple procedure that amounts to post-processing the results of a geometrically linear analysis. The method is inspired by and generalizes Horne's approach (Horne 1963) to estimating the nonlinear response of frames. The present work probes the relationship between the governing nonlinear equations and a hierarchy of approximations. Further, it is shown that an estimate similar to Horne's can be obtained without solving an eigenvalue problem.

The principal result is the extension of Horne's method to the case of nonproportional loading, which generally has more physical significance than proportional loading for structures in wind and earthquake environments. The formulation presented here is distinguished by a clear statements of both the approximations involved and the sense in which the method approximates the exact solution. Qualitative insight into the

<sup>1</sup>Asst. Prof., Univ. of Illinois, 208 N. Romine, Urbana, IL 61801.

<sup>2</sup>Res. Asst., Univ. of Illinois, Urbana, IL 61801.

Note. Discussion open until July 1, 1988. To extend the closing date one month, a written request must be filed with the ASCE Manager of Journals. The manuscript for this paper was submitted for review and possible publication on November 14, 1986. This paper is part of the *Journal of Structural Engineering*, Vol. 114, No. 2, February, 1988. ©ASCE, ISSN 0733-9445/88/0002-0314/\$1.00 + \$.15 per page. Paper No. 22180.

behavior of framed structures is gained both through the success of the approximation as well as through a spectral analysis of the results. The developments clarify the important role of the linearized geometric stiffness matrix in the nonlinear response of frames.

The paper begins with a brief sketch of the essential features of the nonlinear equations governing the response of frame structures. The formula for estimating nonlinear response from geometrically linear response is then derived from a simple decomposition of the nonlinear equations in conjunction with a hypothesis about the way internal forces are distributed in framed structures. A Rankine-type estimate of the limit load is derived for the nonproportional case. Finally, several examples are presented to demonstrate the features of the method. The structures considered include both moment-resisting frames and eccentrically braced frames, range in height from two to eight stories, and are subjected to proportional and nonproportional loads.

### NONLINEAR ANALYSIS OF FRAMES

The equations governing the nonlinear elastic response of planar rods were first presented by Reissner (1972). Simo, Hjelmstad, and Taylor (1984) put the nonlinear equations into a form suitable for numerical analysis by the finite-element method and extended the theory to account for inelasticity of the members. Simo (1982) discusses a consistent second-order approximation to the fully nonlinear rod equations that properly accounts for the effects of shear in elastically deformed beams. These stress-resultant formulations are taken as the point of departure for the present development. The governing nonlinear rod equations will be summarized here. Derivations of the general theory can be found in the cited references.

#### Equilibrium

The equations governing the equilibrium of a beam can be expressed in their weak (variational) form as a statement of the principle of virtual displacements. Accordingly we define the functional

$$G(\mathbf{u}, \boldsymbol{\eta}) = \langle \mathbf{B}(\boldsymbol{\eta}), \boldsymbol{\Xi}(\mathbf{u})\mathbf{R}(\mathbf{u}) \rangle - \langle \boldsymbol{\eta}, \mathbf{q} \rangle \dots\dots\dots (1)$$

in which  $\mathbf{u} = \{u, v, \psi\}^t$  represents the vector of generalized displacements;  $\boldsymbol{\eta}$  = an admissible variation of the displacement field; and the notation  $\langle \boldsymbol{\alpha}, \boldsymbol{\beta} \rangle = \int_{\Omega} \boldsymbol{\alpha}^t \boldsymbol{\beta} ds$  represents the inner product of two vectors  $\boldsymbol{\alpha}$  and  $\boldsymbol{\beta}$  over the entire volume of the structure. The displacement vector  $\{u, v\}$  = the movement of the line of centroids; and  $\psi$  = the rotation of the cross section relative to the initial configuration. In Eq. 1,  $\mathbf{B}(\mathbf{u}) = \{1 + u', v', \psi', \psi\}^t$  is a strain-displacement operator that acts either on the real displacements  $\mathbf{u}$  or their variations  $\boldsymbol{\eta}$ . Note that a prime indicates differentiation with respect to the argument, and a superscript  $t$  indicates the transpose of the argument.  $\mathbf{R} = \{N, V, M\}^t$  is the vector of internal stress resultants;  $N$  = the axial force;  $V$  = the shear force; and  $M$  = the bending moment. The applied loads are designated as  $\mathbf{q} = \{p, q, m\}^t$  where  $p$  = the applied axial force;  $q$  = the applied transverse force; and  $m$  = the applied moment. Concentrated loads can be viewed as limiting cases of distributed loading and thus will not be treated explicitly here. The integral in Eq. 1 is taken

over the entire volume of the structure and is generally accomplished by summing integrals over each element.

The matrix  $\Xi(\mathbf{u})$  in Eq. 1 plays a fundamental role in the nonlinear theory as well as in the developments presented in this paper. The strain gradient operator  $\Xi(\mathbf{u})$  has the physical significance that it reflects the effect of geometry on the equilibrium of the internal resisting forces  $\mathbf{R}$ . Different approximations to nonlinear rod theories are distinguished by different forms of the strain gradient matrix. For example, the geometrically exact theory expressing the Bernoulli-Kirchhoff hypothesis that plane sections remain plane can be expressed as

$$\Xi(\mathbf{u}) = \begin{bmatrix} \cos \psi & \sin \psi & 0 & w' \cos \psi - (1 + u') \sin \psi \\ -\sin \psi & \cos \psi & 0 & -w' \sin \psi - (1 + u') \cos \psi \\ 0 & 0 & 1 & 0 \end{bmatrix} \dots\dots\dots (2)$$

The consistent second-order approximation of Simo (1983) accounting for cross-sectional warping has the following strain gradient matrix:

$$\Xi(\mathbf{u}) = \begin{bmatrix} 1 & (1 - \kappa)v' - \kappa\psi & 0 & \kappa(v' - \psi) \\ -\psi & 1 & 0 & -(1 + u') \\ 0 & 0 & 1 & 0 \end{bmatrix} \dots\dots\dots (3)$$

where  $\kappa$  = the shear coefficient. Note that the consistent second-order strain gradient of Eq. 3 can be obtained by linearization of the fully nonlinear one of Eq. 2 only if  $\kappa = 1$ .

The strain gradient matrix is related to the true nonlinear strain measures in the sense that the virtual strain is defined through the relationship  $\delta\epsilon = D\epsilon \cdot \eta = \Xi'(\mathbf{u})\mathbf{B}(\eta)$ , where  $\epsilon$  is the strain conjugate to  $\mathbf{R}$ . Through standard procedures one can determine the strain displacement equations from this relationship, but since these play a secondary role here they are not presented.

A system is in equilibrium for any configuration,  $\mathbf{u}$ , in which  $G(\mathbf{u}, \eta) = 0$  for any admissible virtual displacement  $\eta$ . Thus,  $G(\mathbf{u}, \eta)$  has the physical significance that it measures, in a weak sense, the equilibrium imbalance in the system. This interpretation will motivate the approximation developed in the next section.

### Constitutive Equations

One can assume an additive decomposition of the strain resultants into an elastic part and an inelastic part,  $\epsilon = \epsilon^e + \epsilon^p$ . The strains are then related to the stress resultants through a rate equation having the form

$$\dot{\epsilon} = \mathbf{D}^{-1}\dot{\mathbf{R}} + \eta \frac{\partial \phi(\mathbf{R})}{\partial \mathbf{R}} \dots\dots\dots (4)$$

where  $\phi(\mathbf{R})$  = the yield potential;  $\eta$  = a scalar multiplier that can be determined from the consistency condition; and  $\mathbf{D} = \text{diag}[EA, \kappa GA, EI] =$  the matrix of elastic moduli. The constitutive relationships are capable of representing generalized yielding due to the interaction of all stress resultants. They can be specialized for particular cross sections and can be extended to incorporate hardening rules by introducing additional internal variables as discussed in Hjelmstad and Popov (1983).

## Numerical Analysis

While it is outside of the scope of the present paper, it should be pointed out that the nonlinear equations just described can be solved through an iterative numerical scheme. The equations of equilibrium can be linearized and discretized using the finite-element method and can be solved using an incremental procedure with Newton-Raphson iteration at each step as described by Simo, Hjelmstad, and Taylor (1984). Ramm (1980) has presented a summary account of algorithms useful for tracing the response of a structure through limit points and into the post-limit regime. The reader is directed to these references and the references contained therein for a more complete account of the exact treatment of the nonlinear equations. The exact numerical analysis is important here only insofar as the examples make use of the exact results for the purpose of comparison. All exact computations presented here were carried out using the procedure described in Simo, Hjelmstad, and Taylor (1984) with a displacement control algorithm as described in Ramm (1980).

## APPROXIMATION OF NONLINEAR LOAD FACTOR

The goal of the present development is to estimate the nonlinear response of a structure from a geometrically linear analysis. In essence we endeavor to find an approximate reduced load factor that gives an estimate of the loads equilibrated by the nonlinear system. Thus, as we trace the linear behavior, we can determine a load factor that estimates the true external loads that the structure can sustain as given by the nonlinear theory.

The development of the approximate approach proceeds as follows. The nonlinear equations are partitioned into a linear part and a nonlinear part. The crucial observation that each configuration satisfying the linear equations is close in form to an associated configuration that satisfies the nonlinear equations then allows an approximation of the internal axial and shear forces. The solution satisfying the geometrically linear equations is substituted into the nonlinear operator. The load factor is then chosen as the one that gives zero equilibrium error in a weak sense.

### Decomposition of Nonlinear Operator

The nonlinear equilibrium functional  $G(\mathbf{u}, \boldsymbol{\eta})$  can be decomposed into a linear part and a nonlinear part. Letting  $\hat{\boldsymbol{\Xi}} = \boldsymbol{\Xi}(\mathbf{u}) - \boldsymbol{\Xi}(\mathbf{0})$  and  $\boldsymbol{\Xi}_0 = \boldsymbol{\Xi}(\mathbf{0})$  we obtain

$$G(\mathbf{u}, \boldsymbol{\eta}) = \langle \mathbf{B}(\boldsymbol{\eta}), \boldsymbol{\Xi}_0 \mathbf{R}(\mathbf{u}) \rangle + \langle \mathbf{B}(\boldsymbol{\eta}), \hat{\boldsymbol{\Xi}}(\mathbf{u}) \mathbf{R}(\mathbf{u}) \rangle - \lambda Q_0 - Q_1 \dots \dots \dots (5)$$

In this equation the virtual work associated with the external loading,  $\langle \boldsymbol{\eta}, \mathbf{q} \rangle$ , has been divided into a fixed part,  $Q_1 = \langle \mathbf{q}_1, \boldsymbol{\eta} \rangle$ , (dead loading) and a proportional part,  $Q_0 = \langle \mathbf{q}_0, \boldsymbol{\eta} \rangle$ , driven by the proportionality factor  $\lambda$ . The expression given by Eq. 5 is a simple restatement of the nonlinear equilibrium equations, which will provide a convenient framework for the following developments.

### Residual at Linear Configuration

Linearizing  $G(\mathbf{u}, \boldsymbol{\eta})$  about the undeformed configuration yields the standard linear equations of equilibrium

$$\langle \mathbf{B}(\boldsymbol{\eta}), \boldsymbol{\Xi}_0 \mathbf{R}(\hat{\mathbf{u}}) \rangle - \lambda Q_0 - Q_1 = 0 \dots \dots \dots (6)$$

One can carry out an analysis with Eq. 6 to obtain a sequence of geometrically linear load factors  $\lambda$  and corresponding linear displacements  $\hat{\mathbf{u}}$ .

Substituting  $\hat{\lambda}$  and  $\hat{\mathbf{u}}$  into the nonlinear operator, the expression for the residual takes the form

$$G(\hat{\mathbf{u}}, \boldsymbol{\eta}) = \langle \mathbf{B}(\boldsymbol{\eta}), \Xi_0 \mathbf{R}(\hat{\mathbf{u}}) \rangle + \langle \mathbf{B}(\boldsymbol{\eta}), \hat{\Xi}(\hat{\mathbf{u}}) \mathbf{R}(\hat{\mathbf{u}}) \rangle - \hat{\lambda} Q_0 - Q_1 \dots \dots \dots (7)$$

**Approximation of Internal Forces**

For many framed structures it can be observed that the distribution of axial forces in a structure does not change appreciably as inelasticity progresses. In contrast, the moment field can change considerably as the structure strains inelastically. The key to the success of the proposed approximation is that the strain gradient operator is linear in the bending moment, and thus  $\hat{\Xi}(\mathbf{u})\mathbf{R}$  does not depend upon the moment. Consequently, the redistribution of moment will not affect the approximation. The internal shear forces will change in accordance with their equilibrium relation to the changing moments. However, the importance of shear is small for most structures. Even for a structure such as the eccentrically braced frame, in which shear plays an important role, only a few of the members are effected by high shear, and thus the aggregate effect of shear on the structure as a whole is small.

In accordance with the foregoing observations we assume that the internal axial forces and shears, designated as  $\hat{\mathbf{R}} = \{N, V\}$ , can be approximately represented in terms of their initial linear values and a proportionality factor as

$$\hat{\mathbf{R}}(\mathbf{u}) = \lambda \hat{\mathbf{R}}_0 + \hat{\mathbf{R}}_1 \dots \dots \dots (8)$$

where  $\hat{\mathbf{R}}_0$  = the vector of internal forces in equilibrium with  $\langle \mathbf{q}_0, \boldsymbol{\eta} \rangle$ ; and  $\hat{\mathbf{R}}_1$  = the vector of internal forces in equilibrium with  $\langle \mathbf{q}_1, \boldsymbol{\eta} \rangle$ . Substituting Eq. 8 into Eq. 7, noting the linearity of  $G(\mathbf{u}, \boldsymbol{\eta})$  with respect to  $\mathbf{R}$ , that  $\langle \mathbf{B}(\boldsymbol{\eta}), \Xi_0 \mathbf{R}_0 \rangle = Q_0$ , and that  $\langle \mathbf{B}(\boldsymbol{\eta}), \Xi_0 \mathbf{R}_1 \rangle = Q_1$ , we obtain

$$G(\hat{\mathbf{u}}, \boldsymbol{\eta}) = (\lambda - \hat{\lambda}) Q_0 + \lambda \langle \mathbf{B}(\boldsymbol{\eta}), \hat{\Xi}(\hat{\mathbf{u}}) \mathbf{R}_0 \rangle + \langle \mathbf{B}(\boldsymbol{\eta}), \hat{\Xi}(\hat{\mathbf{u}}) \mathbf{R}_1 \rangle \dots \dots \dots (9)$$

**Minimizing Residual**

Eq. 9 gives an expression for the magnitude of the residual force at the configuration  $\hat{\mathbf{u}}$  in terms of the single parameter  $\lambda$ . The best value of the parameter is the one that corresponds to the smallest error, i.e.,  $G(\mathbf{u}, \boldsymbol{\eta}) = 0$ . Setting Eq. 9 equal to zero and solving for  $\lambda$ , the following estimate of the actual nonlinear load factor is obtained:

$$\lambda = \frac{\hat{\lambda} Q_0 - \langle \mathbf{B}(\boldsymbol{\eta}), \hat{\Xi}(\hat{\mathbf{u}}) \mathbf{R}_1 \rangle}{Q_0 + \langle \mathbf{B}(\boldsymbol{\eta}), \hat{\Xi}(\hat{\mathbf{u}}) \mathbf{R}_0 \rangle} \dots \dots \dots (10)$$

While Eq. 10 is suitable for computation, it can be recast in a discrete form in terms of the well-known geometric stiffness matrix of the structure. The discrete form has the advantage that it allows comparison with standard structural analysis formulations. In addition, the discrete form exposes the role of the global geometric stiffness matrix. To obtain a convenient discrete representation of Eq. 10, we first truncate a series

expression for  $\hat{\mathbf{E}}(\mathbf{u})\mathbf{R}$  as follows:

$$\hat{\mathbf{E}}(\mathbf{u})\mathbf{R} = \mathbf{A}(\hat{\mathbf{R}})\mathbf{B}(\mathbf{u}) + 0(\mathbf{u}, \mathbf{u}) + \dots \quad (11)$$

where  $\mathbf{A}(\hat{\mathbf{R}})$  = the local-element linearized geometric stiffness matrix. The notation  $0(\mathbf{u}, \mathbf{u})$  stands for the quadratic term in the expansion. Substituting Eq. 11 into Eq. 10 and interpolating the displacements of the structure with a standard finite-element approximation, the expression for the nonlinear load factor takes the discrete form

$$\lambda = \frac{\hat{\lambda}Q_0 - \mathbf{H}'\mathbf{G}_1\dot{\mathbf{U}}}{Q_0 + \mathbf{H}'\mathbf{G}_0\dot{\mathbf{U}}} \dots \quad (12)$$

where  $\mathbf{U}$  and  $\mathbf{H}$  = the discrete nodal displacements and their variations, respectively; and the discrete global geometric stiffness matrices  $\mathbf{G}_0$  and  $\mathbf{G}_1$  are obtained in the standard way from element shape functions and direct assembly procedures. Recall that  $\mathbf{G}_0$  is the linearized geometric stiffness resulting from the action of only the forces  $Q_0$ , whereas  $\mathbf{G}_1$  is the linearized geometric stiffness resulting from the action of only the forces  $Q_1$ .

For the purpose of computing with Eq. 12, it is convenient to characterize the variation in displacements as being proportional to some displaced configuration of the structure  $\mathbf{H} \propto \mathbf{U}$ . An advantage of making the variations proportional to a displacement vector is that one can define a natural way of measuring the displaced configuration of the structure with a scalar quantity, as  $\|\mathbf{U}\|^2 = \mathbf{U}'\mathbf{G}\mathbf{U}$ . In general  $\mathbf{G}$  is not guaranteed to be positive-definite, and thus  $\|\mathbf{U}\|$  does not define a true norm. However, it does have the advantage of treating the displacements in a dimensionally consistent manner, and we adopt it here as the measure of the deformed state of the structure. An objective measure of displacement such as  $\|\mathbf{U}\|$  is especially desirable for irregular structures where it is not clear that a measure such as displacement at a single point is most representative of the deformation of the structure.

Eq. 12 with  $\mathbf{H} = \mathbf{U}$  provides us with a formula for computing the nonlinear load factor from the sequence of linear configurations generated from Eq. 6. The second term in the numerator of Eq. 12 vanishes in the absence of dead loading.

### Spectral Analysis

Eq. 12 can be studied through a spectral analysis of the system. The spectral approach provides an enlightening framework for characterizing the behavior of complex systems by significantly reducing the number of important response parameters. By projecting the displacement response of a structure onto an associated eigenbasis, we need only follow the progress of a few generalized components of the system to understand the behavior of that system. The spectral analysis will help in our evaluation of the approximations we have made. Another benefit of performing a spectral analysis is the ready identification of the special case examined by Horne (1963).

Consider the eigenvalue problem defined by the initial elastic and geometric stiffness matrices of the structure:

$$\mathbf{K}\phi = \mu\mathbf{G}\phi \dots \quad (13)$$

where  $\mathbf{K}$  = the initial elastic stiffness matrix; and  $\mathbf{G}$  = the geometric stiffness matrix of the system. A discrete system with  $n$  degrees-of-freedom will yield  $n$  eigenpairs satisfying Eq. 13. In accordance with standard practice, the eigenpairs are ordered such that  $|\mu_1| < |\mu_2| < \dots < |\mu_n|$ , and the eigenvectors are normalized such that  $\phi_i^T \mathbf{G} \phi_j = \delta_{ij}$ , where  $\delta_{ij}$  = the Kronecker delta.

For proportionally loaded structures, there is only one initial geometric stiffness and thus only one associated eigenvalue problem. A nonproportionally loaded structure, on the other hand, has one associated eigenvalue problem corresponding to the proportional loads ( $\mathbf{G}_0$ ) and one corresponding to the dead loads ( $\mathbf{G}_1$ ). We will consider that the nonproportional load case gives rise to a family of associated eigenvalue problems with  $\mathbf{G} = \epsilon \mathbf{G}_0 + \mathbf{G}_1$ , in which  $\epsilon$  = the parameter of the family. As  $\epsilon \rightarrow 0$ , the eigenvalue problem is governed by dead loads only. As  $\epsilon \rightarrow \infty$ , the eigenvalue problem is governed by proportional loads only. We will see in the examples that the specific choice of  $\epsilon$  is crucial to the success of some of the approximations.

Let the displacement vector  $\mathbf{U}$  be decomposed into its components along the eigenbasis induced by the eigenvalue problem Eq. 13. The displacements can then be expressed in terms of spectral ordinates as

$$\mathbf{U} = \sum_{i=1}^n \alpha_i \phi_i \dots \dots \dots (14)$$

We will identify the  $\alpha_i$  as being modal participation factors, measuring the components of displacement relative to the basis  $\{\phi_i\}$ . The participation factors can be computed from the displacement  $\mathbf{U}$  using the formula

$$\alpha_i = \frac{\mathbf{U}_i^T \mathbf{G} \phi_i}{\phi_i^T \mathbf{G} \phi_i}; \quad i = 1, \dots, n \dots \dots \dots (15)$$

where  $\mathbf{G}$  = the metric of the space spanned by the eigenvectors. If the basis  $\{\phi_i\}$  is normalized with respect to the metric  $\mathbf{G}$ , then the denominator of Eq. 15 is unity.

Substituting Eq. 14 into the expression for the nonlinear load factor (Eq. 12), noting that  $\mathbf{Q}_0 = \mathbf{U}^T \mathbf{R}_0 = \mathbf{U}^T \mathbf{K} \mathbf{U}_0$ , one obtains the following expression:

$$\lambda = \frac{\hat{\lambda} \sum \alpha_{0i} \alpha_i \mu_i - \sum \sum \alpha_i \alpha_j \gamma_{ij}^1}{\sum \alpha_{0i} \alpha_i \mu_i + \sum \sum \alpha_i \alpha_j \gamma_{ij}^0} \dots \dots \dots (16)$$

where  $\alpha_{0i}$  = the initial linear participation factors, i.e.  $\mathbf{U}_0 = \sum \alpha_{0i} \phi_i$ ; and  $\mu_i$  = the eigenvalues of Eq. 13. We have noted in the above expression that the eigenvalue problem has been normalized such that  $\phi_i^T \mathbf{G} \phi_j = \delta_{ij}$ . Since  $\mathbf{G}$  need not (but could) be either  $\mathbf{G}_0$  or  $\mathbf{G}_1$ , we define the parameters  $\gamma_{ij}^0 = \phi_i^T \mathbf{G}_0 \phi_j$  and  $\gamma_{ij}^1 = \phi_i^T \mathbf{G}_1 \phi_j$ .

If first-mode behavior is assumed to dominate, i.e.,  $\alpha_1 \neq 0$ ,  $\alpha_i = 0$ ,  $i = 2, \dots, n$ , then under these restrictions we have

$$\lambda(\alpha) = \frac{\hat{\lambda}(\alpha) \alpha_0 \mu - \alpha \gamma_1}{\alpha_0 \mu + \alpha \gamma_0} \dots \dots \dots (17)$$

where the subscripts on  $\alpha$ ,  $\alpha_0$ , and  $\mu$  are understood to be one;  $\gamma_0 = \gamma_{11}^0$ ; and  $\gamma_1 = \gamma_{11}^1$ . Note also that an approximation having the form of Eq. 17

can be achieved using any of the eigenvectors in the expression for the nonlinear load factor. This observation is important because the fundamental mode will not always dominate the limit response of the frame.

Eq. 17 degenerates to the expression given by Horne (1963) if only proportional loads are considered ( $\gamma_1 = 0, \gamma_0 = 1$ ). Horne has suggested that Eq. 17 provides a lower bound on the nonlinear load factor for moment-resisting frames. However, as demonstrated in one of the examples, we find that the lower bound character can be spoiled if the selected mode does not actually dominate the response.

If the displacement of the structure is approximated as proportional to a constant vector,  $\mathbf{U} = \alpha \mathbf{v}$  (not an eigenvector), the preceding derivations apply, except that  $\mu$  is simply the Rayleigh quotient and not an eigenvalue. The ramifications of choosing the vector  $\mathbf{v}$  to be the initial displaced configurations of the structure under load ( $\mathbf{U}_0$ ) will be examined in the examples later. One might expect that when the chosen assumed shape is representative of the shape at the limit load, then a good estimate of the limit load can be achieved. Such an approximation has the computational advantage of avoiding the solution of an eigenvalue problem.

### Rankine-Type Formula for Limit Load

The limit load plays a singularly significant role in the limit design of structures. Thus, its estimation is of fundamental importance. Indeed, plastic design is predicated on the knowledge of the "limit" load without knowledge of the response history. We demonstrate in this section that the limit load can be estimated from Eq. 17, i.e., by assuming that the displaced configuration is controlled by a single parameter. The success of the estimate relies both on an appropriate choice of the displaced shape and on the invariance of that shape as the deformation progresses. The spectral analyses of the example structures presented later will shed light on the validity of the estimate.

The limit load occurs when  $\lambda'(\alpha) = 0$ . Taking the derivative of Eq. 17 with respect to  $\alpha$  and setting the resulting expression equal to zero, one obtains an expression from which the limit displacement  $\bar{\alpha}$  can be evaluated. Carrying out this operation we obtain the expression

$$(\alpha_0 \mu + \alpha \gamma_0) \lambda'(\alpha) - \gamma_0 \lambda(\alpha) - \gamma_1 = 0 \quad (18)$$

the solution of which defines the limit displacement  $\bar{\alpha}$ . Substituting Eq. 18 into Eq. 17 we arrive at an approximation of the limit load in terms of the slope of the linear response curve evaluated at the limit displacement

$$\lambda_{cr} = \frac{1}{\gamma_0} [\alpha_0 \mu \lambda'(\bar{\alpha}) - \gamma_1] \quad (19)$$

If only proportional loading is considered ( $\gamma_1 = 0, \gamma_0 = 1$ ), then Eq. 19 reduces to

$$\lambda_{cr} = \alpha_0 \mu \lambda'(\bar{\alpha}) \quad (20)$$

which is the formula given by Horne (1963). Thus, Eq. 19 generalizes Horne's formula to the case of nonproportional loading.

For some structures, the transition from elastic to plastic behavior covers a reasonably short range of displacement values, as shown in Fig.

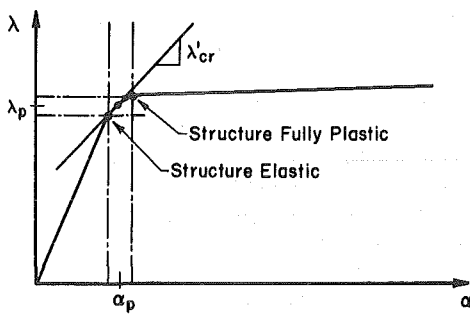


**FIG. 1. Idealized Structural Behavior for Rankine-Type Estimate**

1. As the structure passes through this region the slope  $\lambda'$  changes dramatically from the large, elastic slope to a very small, post-yield slope. The critical value of the slope,  $\lambda'(\bar{\alpha})$  is almost certainly contained within these bounds. For these structures, failure will occur at or near the "knee" of the linear curve, which has an approximately identifiable displacement  $\alpha_p$  and load level  $\lambda_p$  (the linear plastic capacity of the structure). The known values of force and displacement can be substituted into Eq. 18 to solve for the indeterminate slope  $\lambda'$ . Accordingly, we obtain

$$\lambda' \approx \frac{\gamma_1 + \gamma_0 \lambda_p}{\alpha_0 \mu + \gamma_0 \alpha_p} \dots\dots\dots (21)$$

Substituting this value into Eq. 19 one obtains an estimate of the limit load. Noting that  $\alpha_p = \alpha_0 \lambda_p$ , the estimate can be expressed as

$$\lambda_{cr} \approx \lambda_p \frac{\mu - \gamma_1}{\mu + \gamma_0 \lambda_p} \dots\dots\dots (22)$$

Again, if we assume proportional loading, Eq. 22 reduces to the so-called Merchant-Rankine load of the structure

$$\lambda_R = \frac{\mu \lambda_p}{\mu + \lambda_p} \dots\dots\dots (23)$$

where  $\mu$  = the eigenvalue corresponding to  $\phi$ .

**APPLICATIONS TO FRAMED STRUCTURES**

The remainder of the paper is devoted to application of the methods derived previously to a set of examples. The examples will serve to demonstrate the effectiveness of the approximate methods of tracing the limit behavior of framed structures and to indicate the limitations of the approximate formulas. Also, the examples will demonstrate that the approximate methods provide a useful framework for assessing the limit performance of framed structures in general. Thus, we get insight both into the performance of the method and into the behavior of framed structures.

Six structures have been analyzed. These structures cover a wide range of framed structure types including moment-resisting and eccentrically

TABLE 1. Member Properties

Section (1)	Stiffness Properties ( $\times 10^{-3}$ )			Yield Properties		
	EA (k) (2)	$\kappa GA$ (k) (3)	EI (k-ft <sup>2</sup> ) (4)	$N_o$ (k) (5)	$V_o$ (k) (6)	$M_o$ (k-ft) (7)
W14×43	365	183	86.2	449	83	206.3
W14×48	410	205	97.2	510	90	233.3
W14×53	425	226	108.9	560	102	260.4
W14×132	1,125	563	308.1	1,409	183	710.0
W14×426	3,625	1,813	1,329	4,705	610	2,726
ST 8×8×(5/16)	270	135	18.3	340	100	83.3
"Column"	1,200	600	208.3	1,650	500	583.3

Note: 1 k = 4.448 kN; 1 ft = 0.3048 m.

braced frames, low-rise and high-rise buildings, and proportionally and nonproportionally loaded structures. The designation used for the examples describes the framing type (MRF means moment-resisting frame and EBF means eccentrically braced frame). The properties of most of the members used in the example structures are summarized in Table 1.

Each structure is submitted to an exact nonlinear analysis using the methodology and finite elements developed in Simo, Hjelmstad, and Taylor (1984). For each of these "exact" analyses, the solution has been decomposed into components along the eigenbasis  $\{\phi_i\}$ , where the basis vectors are generated from the eigenvalue problem defined by Eq. 13. with  $G$  selected from the family of initial geometric stiffness matrices. The modal participation factors  $\alpha_i$  are computed according to Eq. 15.

Tracing the history of the modal participation factors as the nonlinear solution progresses allows one to assess the change in the character of the displaced configuration as the nonlinearities accrue. One can also compare different bases by seeing how the same nonlinear response curve reflects on each basis. Viewing the results in this way gives an indication as to why the approximate methods work well in some cases but not in others. A modal decomposition gives a good qualitative representation of the progress of the solution.

For each structure, the nonlinear load versus displacement history is presented for several cases: (1) The actual computed nonlinear response (designated as "Exact Nonlinear" in the figures); (2) the actual computed response without nonlinear geometric effects (designated as "Exact Linear" in the figures); (3) an approximation to the nonlinear response using Eq. 12; and (4) an approximation of the nonlinear response using Eq. 17.

The finite elements used in these analyses were all  $C^0$  quadratic elements. Each structural member was discretized using two of these elements. Inelasticity of the elements accrues due to the interaction of shear force, axial force, and bending moment. The computational model is a viscoplastic penalty approach to model-perfect elastoplasticity. The yield potential used in these computations was

$$\phi(n, v, m) = |m| + n^2(1 + v^2) + v^4 - 1 \dots\dots\dots (24)$$

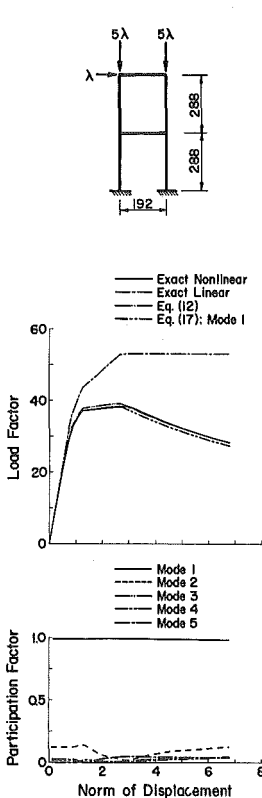


FIG. 2. Response of MRF-1

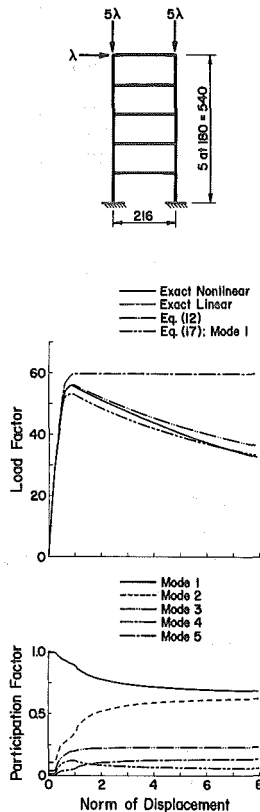


FIG. 3. Response of MRF-2

where  $n = N/N_0$ ,  $v = V/V_0$ , and  $m = M/M_0$  are the axial force, shear force, and bending moment normalized by their fully plastic values. Each stage of the computation is iterated to satisfaction of equilibrium to within a specified tolerance on the Euclidean norm of the out-of-balance forces. The following paragraphs discuss the results of the analyses.

MRF-1 is a two-story, single-bay, moment-resisting frame with tall stories. The beam members are  $W14 \times 53$  and the columns are of type "column." The structure was proportionally loaded as shown in the figure, with two vertical loads of magnitude  $5\lambda$  and one lateral load of magnitude  $\lambda$  applied at the top level. The results of the various analyses of MRF-1 are shown in Fig. 2, along with the spectral decomposition of the exact nonlinear solution.

The linear elastoplastic response of the structure shows a typical multilinear force-deformation behavior, with the changes in slope corresponding to the formation of plastic zones in the structure. Due to the relatively heavy vertical loads, the actual capacity of the structure is greatly reduced from the linear "collapse load." Both Eq. 17 and Eq. 12 give excellent approximations of the nonlinear behavior of the frame. Note in particular the accuracy with which the post-limit behavior of the frame

is traced by the approximate methods. Upon examining the evolution of modal participation factors of the actual response, one can see that the first buckling mode dominates the response throughout the analysis.

MRF-2 is a five-story, single-bay frame with  $W14 \times 53$  beams and  $W14 \times 48$  columns. The loading of the frame was similar to that of MRF-1 with loading at the top level. The response of MRF-2 is shown in Fig. 3. Again, both approximate methods work well. Eq. 12 gives a more accurate assessment of the response near the limit load than does Eq. 17. Note that because the columns are not as slender as the ones in MRF-1, the reduction in carrying capacity due to geometric effects is not as dramatic as it was for MRF-1. However, the slope of the post-limit response curve is steeper, indicating poorer post-limit behavior. One can note that while the initial response tends to be dominated by the first mode, the second mode contributes more as the structure settles into its final collapse deformation mode.

MRF-3 is also a moment-resisting frame and has the same topology as MRF-1. This structure is different from the previous structures in that the vertical loads are gravity loads instead of proportional loads. The lateral loads at the two-story levels were equal and increased monotonically in accordance with a proportionality factor. Such a loading would be representative of a building structure subjected to earthquake or wind loads.

The response of the structure to the imposed loading is shown in Fig. 4. Note that the initial displacement is due to the presence of dead loading, while the proportionality factor is still zero. Two different approximations within the context of Eq. 12 are shown in Fig. 4(a). The approximations differ only in the choice of the form of the variation in displacements  $\mathbf{H}$ . In one case,  $\mathbf{H}$  is taken to be proportional to the initial displaced configuration  $\mathbf{U}_0$ , while in the other case, it is taken to be proportional to the current displacement  $\mathbf{U}$ . Both approximations give good results but demonstrate that the method depends upon the choice of the vector representing the variation in displacements.

The results obtained from Eq. 17 are shown in Fig. 4(b and c). Three different methods of calculation were used: (P)  $\alpha$  and  $\{\mu, \phi\}$  computed using only the proportional part of the geometric stiffness; (D)  $\alpha$  and  $\{\mu, \phi\}$  computed using only the dead part of the geometric stiffness; and (P + D)  $\alpha$  and  $\{\mu, \phi\}$  computed using a geometric stiffness  $\mathbf{G} = \lambda_{cr} \mathbf{G}_0 + \mathbf{G}_1$ , where  $\lambda_{cr}$  = the actual limit load of the structure. Case (P + D) works well for this problem whereas cases (P) and (D) do not. The reason that the first two cases performed so poorly can be seen upon examining the evolution of the modal participation factors. Three different versions of this history are shown in Fig. 4(d-f), corresponding to the geometric stiffness matrices and associated eigenvectors of cases (P), (D), and (P + D). The first (P) eigenvector contributes very little to the response. The first (D) eigenvector is totally orthogonal to the displaced configuration of the structure. Eq. 17 was also tried using mode five for the (P) case and mode six for the (D) case. The results for these cases were also poor. It is interesting to note that, while mode one of the (P) and (D) cases did not contribute to the response, mode one of the (P + D) case dominated the response as it passed through the limit load. The obvious shortcoming of the method represented by case (P + D) is that the limit load is not known a priori. However, one could estimate the limit load from a Rankine approximation

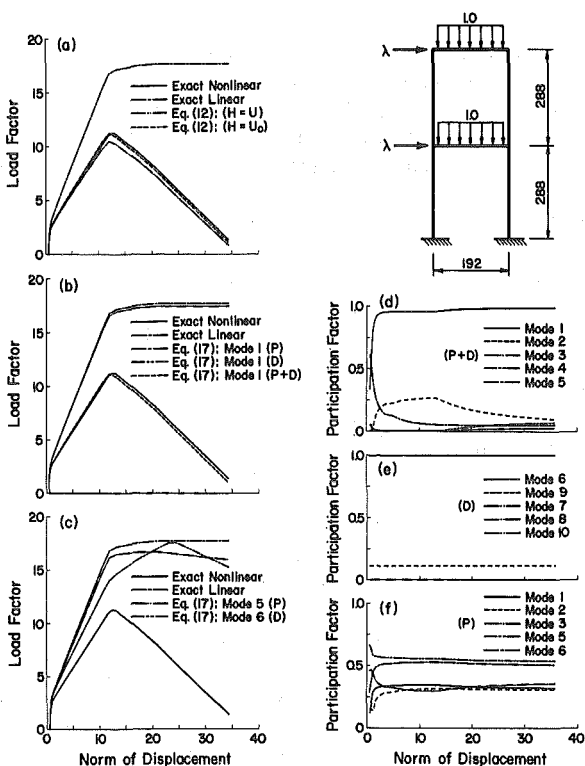


**FIG. 4. Response of MRF-3: (a) Estimates Based on Eq. 12; (b) Estimates Based on Eq. 17 Using Mode One; (c) Estimates Based on Eq. 17 Using Other Modes; (d) Evolution of Participation Factors: (P + D) Case; (e) Evolution of Participation Factors: (D) Case; (f) Evolution of Participation Factors: (P) Case**

before embarking on the solution. The method that uses Eq. 12 does not suffer from the ambiguities that Eq. 17 does and does not presuppose a priori knowledge of the limit load.

One can conclude that it is not the vector  $\mathbf{v}$  that is important to the approximation, but the metric  $\mathbf{G}$  used in computing the norm of the displacements. To verify this conclusion, the initial displacement  $\mathbf{v} = \mathbf{U}_0$  was used in Eq. 17 with the (P + D) geometric stiffness. The results for this case were found to be indistinguishable from the curve  $\mathbf{H} = \mathbf{U}_0$  shown in Fig. 4(a).

MRF-4 is an eight-story, single-bay frame similar to the one analyzed by Korn and Galambos (1968). Similarly to MRF-3, this frame was subjected to nonproportional loads. The member designations are given in Table 2. The loading is shown in Fig. 5, along with the response of the structure. MRF-4 was subjected to the same analyses as was MRF-3.

One can see from Fig. 5(a) that Eq. 12 approximates the true solution well. As was true with MRF-3, Eq. 17 gives meaningful results only for the case (P + D) where the geometric stiffness matrix has  $\epsilon$  equal to the limit load of the structure. Contrary to MRF-3, this structure has a good result

TABLE 2. Frame MRF-4 Properties

Story (1)	Column (2)	Beam (3)
1	W14×99	W14×38
2	W14×90	W14×34
3	W12×79	W14×30
4	W10×49	W12×26
5	W8×35	W12×22
6	W8×31	W10×22
7	W8×31	W8×21
R	W6×20	W8×18

for case (D) in which only dead loads were used for the geometric stiffness. The reason for this is clear upon reviewing the modal participation histories for the various cases shown in Fig. 5(d and e). The case (D) shows a history of modal participation factors almost identical to the (P + D) case. The first proportional mode does not contribute significantly to the

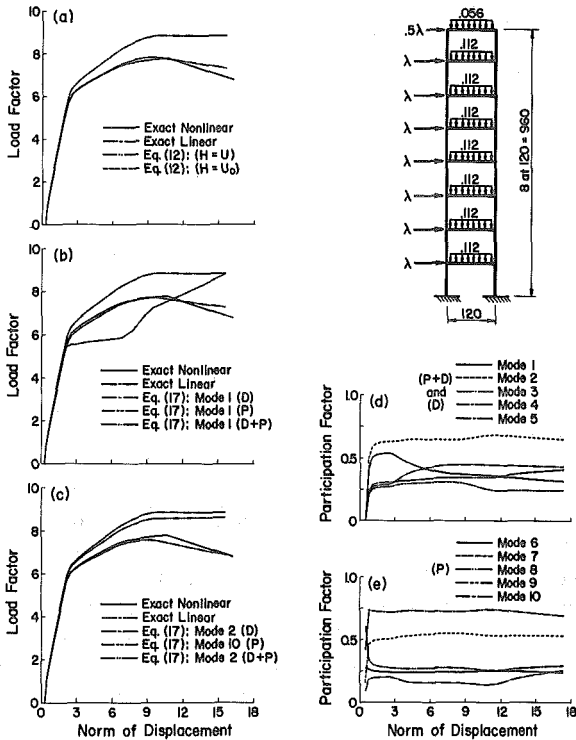
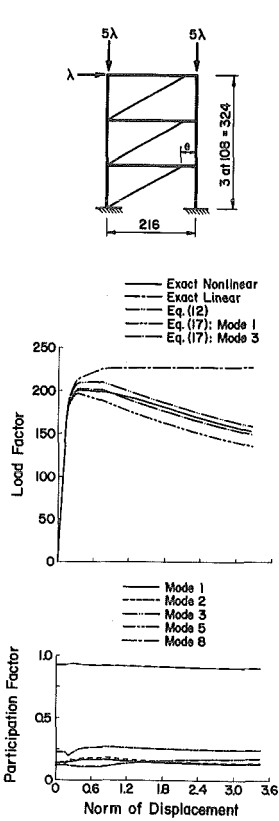
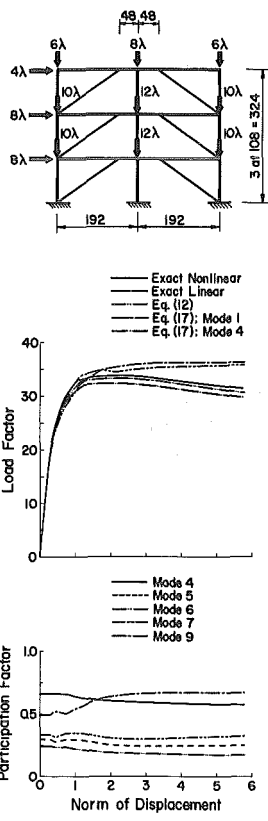


FIG. 5. Response of MRF-4: (a) Estimates Based on Eq. 12; (b) Estimates Based on Eq. 17 Using Mode One; (c) Estimates Based on Eq. 17 Using Other Modes; (d) Evolution of Participation Factors: (P + D) and (D) Cases; (e) Evolution of Participation Factors: (P) Case



**FIG. 6. Response of EBF-1**



**FIG. 7. Response of EBF-2**

response. The success of the case (D) can be considered coincidental. Again the initial displacement  $v = U_0$  was used in conjunction with the (P + D) case and was found to give excellent results.

EBF-1 is a three-story, single-bay, eccentrically braced frame with an eccentricity  $e = 22$  in. (0.56 m). The frame was subjected to proportional loads at the top level. The various computed responses of the frame to the applied loading is shown in Fig. 6. One can see that both approximate methods give a reasonable representation of the actual nonlinear behavior. Eq. 12 slightly overestimates the response, while Eq. 17 slightly underestimates the response. Both methods accurately reproduce the post-limit slope of the response curve, and thus give an accurate representation of the rate of loss of carrying capacity of the structure. The method based upon Eq. 17 can be improved by noting that the structure responds predominantly in the third mode. The result of using the third mode in Eq. 17 is also shown in Fig. 6.

EBF-2 is a three-story, two-bay, eccentrically braced frame having  $W14 \times 43$  beams,  $ST8 \times 8 \times (5/16)$  braces, and  $W14 \times 132$  columns except for the bottom-story interior column which is a  $W14 \times 426$  section. The

TABLE 3. Summary of Results

Frame (1)	Approximate $\lambda_{cr}/$ Exact $\lambda_{cr}$ (2)	Normalized Rankine Estimates of Limit Load		Approximate $\Delta_{cr}/$ Exact $\Delta_{cr}$ (5)
		$v = U_0$ (3)	$v = \phi_1$ (4)	
MRF-1	1.009	1.187	1.164	0.881
MRF-2	1.001	1.041	1.004	1.000
MRF-3	0.997	1.412	1.407	0.942
MRF-4	1.005	1.095	1.064	0.916
EBF-1	1.045	1.123	1.086	1.499
EBF-2	0.984	1.047	0.998	0.929

loading was proportional as shown in Fig. 7, which also shows the response curves of the structure. One can see that Eq. 12 gives good results for this structure.

An interesting feature of the response of this structure is that modes four through nine were the greatest contributors to the displacement field. In addition, modes four and nine shift in importance as the deformations progress. The computations using Eq. 17 were carried using mode one, four, and nine. It is clear that use of mode one does not give good results, and, in fact, violates the lower-bound character suggested by Horne. Using either mode four or mode nine gives a better representation of the response than mode one.

### Summary of Examples

A summary of the approximation of the limit loads and displacements of the example structures are shown in Table 3. The limit load of the structures computed from Eq. 12 was within 5% for all cases and was better for most of the cases. The estimate of the limit drift  $\Delta_{cr}$  was also accurately predicted by Eq. 12.

Table 3 also contains two Rankine estimates of the limit load, one based upon the fundamental eigenvector  $v = \phi_1$  and one based upon the initial displacement  $v = U_0$ . The values presented are the ratio of the Rankine estimate to the true limit load of the structure. Except for MRF-4, the estimate of the limit load is reasonably good. Almost all values give an overestimate of the limit load. While the Rankine estimate based upon the eigenvector is uniformly better than the one based upon the initial displacement, there is really no appreciable difference between the two. Either one might be used as an estimator of the limit load for use in nonproportional load cases with Eq. 17.

### CONCLUSIONS

An approximate method for tracing the limit and post-limit response of framed structures has been presented. The method was constructed from the weak form of the nonlinear equations of equilibrium in conjunction

with some observations on the behavior of framed structures. Several example structures having different topologies and loading conditions were analyzed to demonstrate the effectiveness of the method.

The importance of the approximate method presented is not so much its potential for post-processing geometrically linear analyses, but rather the qualitative information it gives into the behavior of framed structures. Eq. 12 clearly distinguishes the manner in which nonlinear geometry affects the limit and post-limit response of the structure both for proportional and nonproportional loads. The approximate method and the subsequent spectral analyses of the examples demonstrate the role of the geometric stiffness matrix in the nonlinear response and clarify the issue for the nonproportional load case.

While Eq. 17 allows all solution parameters to be estimated from the initial state, it suffers from the difficulty of not knowing the dominant mode in advance, and applies to nonproportionally loaded structures only if the geometric stiffness matrix is chosen with  $\epsilon$  equal to the limit load of the structure. An estimate of the limit load for use in this equation might be obtained from a Rankine-type formula. It has further been observed that the eigenvector  $\phi$  plays a secondary role in Eq. 17. Good results can be obtained using the initial displaced configuration of the structure with a Rayleigh-quotient estimate of the eigenvalue, obviating the need to solve an eigenvalue problem. Contrary to Horne's hypothesis, Eq. 17 does not give a lower bound to the solution if a poor choice is made for the selected eigenvector, even for proportionally loaded structures.

## APPENDIX I. REFERENCES

- Ariaratnam, S. T. (1961). "The Southwell method for predicting critical loads of elastic structures." *Q. J. Mech. Appl. Math.*, 14(2), 137-154.
- Hjelmstad, K. D., and Popov, E. P. (1983). "Seismic behavior of active links in eccentrically braced frames." *Report No. UCB/EERC-83/15*, University of California, Berkeley, Calif.
- Horne, M. R. (1963). "Elasto-plastic failure loads of plane frames." *Proc. R. Soc. London*, 274(1358), 343-364.
- Horne, M. R., and Merchant, W. (1965). *The stability of frames*, Pergamon Press, New York, N.Y.
- Horne, M. R. (1962). "The effect of finite deformations in elastic stability of plane frames." *Proc. R. Soc. London Ser. A*, 266(1324), 47-68.
- Korn, A., and Galambos, T. V. (1972). "Behavior of elastic-plastic frames." *J. Struct. Div.*, ASCE, 94(ST5), 1119-1141.
- McNamee, B. M., and Lu, L.-W. (1972). "Inelastic multistory frame buckling." *J. Struct. Div.*, ASCE, 98(ST7), 1613-1631.
- Ramm, E. (1980). "Strategies for tracing nonlinear response near limit points." *Europe-U.S. Workshop on nonlinear finite element analysis in structural mechanics*, Bochum, West Germany.
- Reissner, E. (1972). "On one-dimensional finite-strain beam theory: the plane problem." *J. Appl. Math. Phys.*, 23(5), 795-804.
- Simo, J. C. (1982). "A consistent formulation of nonlinear theories of elastic beams and plates." *Report No. UCB/SESM-82/06*, University of California, Berkeley, Calif.
- Simo, J. C., Hjelmstad, K. D., and Taylor, R. L. (1984). "Numerical formulations of elasto-viscoplastic response of beams accounting for the effect of shear." *Comput. Methods Appl. Mech. Eng.*, 42(3), 301-330.

## APPENDIX II. NOTATION

The following symbols are used in this paper:

$\mathbf{B}$	=	strain displacement operator;
$\mathbf{D}$	=	elastic moduli;
$\mathbf{G}, \mathbf{G}_0, \mathbf{G}_1$	=	geometric stiffness matrices;
$\mathbf{H}$	=	variation of discrete nodal displacements;
$\mathbf{K}$	=	initial elastic stiffness matrix;
$M$	=	bending moment;
$m$	=	applied moment;
$N$	=	axial force;
$p$	=	applied axial force;
$Q, Q_0, Q_1$	=	virtual work of external loads, proportional load, dead load;
$\mathbf{q}$	=	applied forces;
$q$	=	applied transverse force;
$\mathbf{R}$	=	internal resisting forces;
$\hat{\mathbf{R}}, \hat{\mathbf{R}}_0, \hat{\mathbf{R}}_1$	=	internal shear and axial forces, proportional load, dead load;
$\mathbf{u}$	=	cross-section displacements;
$u$	=	axial displacements;
$V$	=	shear force;
$\mathbf{v}$	=	displaced shape vector;
$v$	=	transverse displacements;
$\alpha_{0i}, \alpha_i$	=	displacement modal participation factors;
$\gamma_0, \gamma_1$	=	parameters;
$\delta_{ij}$	=	Kronecker delta;
$\boldsymbol{\varepsilon}, \boldsymbol{\varepsilon}^e, \boldsymbol{\varepsilon}^p$	=	strain resultants;
$\boldsymbol{\eta}$	=	admissible variation of displacement field;
$\kappa$	=	shear coefficient;
$\lambda, \lambda^{\circ}, \lambda_{cr}$	=	proportional load factor, linear load factor, limit load;
$\mu, \mu_i$	=	elastic critical eigenvalue;
$\boldsymbol{\Xi}$	=	strain gradient;
$\boldsymbol{\Phi}_i$	=	eigenvector;
$\phi(\mathbf{R})$	=	yield potential of member;
$\psi$	=	rotation displacements; and
$\Omega$	=	volume of structure.